# HIGHER ORDER STATISTICS AND SPECTRA ANALYSIS OF SLEEP SPINDLES

*Tayfun Akgül*†, *Mingui Sun*‡, *Robert J. Sclabassi*‡ *and A. Enis Çetin**

†Electrical and Computer Engineering Department
Drexel University, Philadelphia PA, 19104

‡Laboratory for Computational Neuroscience
Department of Neurological Surgery
University of Pittsburgh PA, 15261

*Department of Electrical Engineering
Bilkent University, Ankara, Turkey

**ABSTRACT**

In this paper we analyze sleep spindles, observed in EEG recorded from humans during sleep, using both time and frequency domain methods which depend on higher order statistics and spectra. The time domain method combines the use of second and third order correlations to reveal information on the stationarity of periodic spindle rhythms, detecting transitions between multiple activities. The frequency domain method, based on the normalized bispectrum, describes the frequency interactions associated with the second order nonlinearities occuring in the observed EEG. Results for real data are presented.

## 1. INTRODUCTION

The EEG is a continuous time-varying voltage, reflecting ongoing functional activity in the brain [1]. EEG activity typically has amplitudes from 10 to $100\mu V$ and a frequency content of from $0.5$ to $40$ Hz. Signals of 10 to $30\mu V$ are considered low amplitude and potentials of 80 to $100\mu V$ are considered high amplitude. EEG is traditionally divided into four bands: $\delta$ from 0 to 4 Hz, $\theta$ from 4 to 8 Hz, $\alpha$ ranging 8 to 13 Hz and $\beta$ from 13 to 30 Hz. An alert person displays a low amplitude EEG of mixed frequencies in the 13 to 18 Hz range, while a relaxed person produces large amounts of sinusoidal waves, at a single frequency in the 8 to 13 Hz range which are particularly prominant at the back of the head.

Adult human sleep, for which several models have been proposed [2], is classified into waking (W), quiet sleep (QS), and rapid eye movement (REM) stages. QS is further differentiated into four stages on the basis of brain, muscle, and eye activity. QS, REM, and occasional momentary wakings occur in a periodic sequence throughout the night, taking approximately 90 min in the adult. There is some suggestion that this alteration of W, QS, and REM is a manifestation of a basic rest/activity cycle characterized by periods of relative activity and action alternating with periods of relative inactivity and fantasy over the entire day.

As an individual goes to sleep, alpha activity is replaced by a lower amplitude, mixed frequency voltage (stage 1 QS), which within minutes has superimposed 1- to 2-s bursts of 12 to 14 Hz activity called sleep spindles (stage 2, QS). Spindle activity can be considered as oscillations and noise-free sleep spindle waveforms may exhibit periodic, quasiperiodic or complex oscillations. Earlier studies [3, 4] have shown that there coexist two types of spontaneous spindle waves. In more recent work [5], it has been shown, by using matched filtering techniques, that one of these activities is centered around 12 Hz and the other around 14 Hz. In a recent study, Sun *et al.,* [6] localized spindle activity in the brain via time-frequency analysis and synthesis of EEG, and showed that the origin of this activity is in the area of thalamus in humans, which is in agreement with previous data from the cat [4].

In this paper we apply higher order statistical measures both in the time and frequency domains to investigate the spindle activity associated with stage 2 sleep. While the time domain techniques, which depend on the combination of second and third order statistics to trace the oscillatory dynamics of the waveforms around spindle activity, are used to investigate the nonstationary behavior of the spindles, the frequency domain method is used to investigate frequency interactions related to nonlinear properties of the central nervous system. Note that some earlier EEG analysis using higher-order statistics and spectra can be found in [7]-[11].

## 2. HIGH-ORDER STATISTICS OF SIGNAL

Autocorrelation function, $R(\tau) = E[x(n)x(n+\tau)]$, for wide-sense stationary signal $x(n)$, is widely used in signal processing. However, it suppresses the phase relationships of these components. This loss of information can be important if there exists phase couplings due to nonlinearities in the signal of interest. Phase information is preserved when the order of the spectra is greater than two [12]. The autotriplecorrelation function (third order statistics) $c(\tau_1, \tau_2)$ of $x(n)$ is defined as [13]:

$$c(\tau_1, \tau_2) = E[x(n)x(n+\tau_1)x(n+\tau_2)], \qquad (1)$$

and the 2-D Fourier transform of this equation, the bispectrum of the signal $x(n)$, is expressed by

$$B(\omega_1, \omega_2) = \sum_{\tau_1} \sum_{\tau_2} c(\tau_1, \tau_2) e^{-j\omega_1\tau_1} e^{-j\omega_2\tau_2}. \qquad (2)$$

It can be shown [13] that the bispectrum in (2) can be written as

$$B(\omega_1, \omega_2) = A(\omega_1)A(\omega_2)A^*(\omega_1 + \omega_2) \qquad (3)$$

where $^*$ denotes complex conjugate, and $A(\omega)$ is the discrete Fourier transform of $x(n)$.

For a stochastic process $x(n)$, $B(\omega_1, \omega_2)$ is a random variable. Its expected value is given by

$$\bar{B}(\omega_1, \omega_2) = E[A(\omega_1)A(\omega_2)A^*(\omega_1 + \omega_2)] \tag{4}$$

and the normalized bispectrum (also referred to as bicoherence, second order coherency, bicoherency index, etc.,) [13]:

$$b^2(\omega_1, \omega_2) = \frac{|\bar{B}(\omega_1, \omega_2)|^2}{\bar{P}(\omega_1)\bar{P}(\omega_2)\bar{P}(\omega_1 + \omega_2)} \tag{5}$$

where $\bar{P}(\omega) = E[A(\omega)A^*(\omega)]$. $b^2(\omega_1, \omega_2)$ is a useful tool for detecting and characterizatin nonlinearities [14], i.e., quadratically couplings.

If $x(n)$ is a periodic sequence with period $p$, then $R(\tau)$ is also periodic. In speech analysis problems, (for example, pitch period estimation) a widely used technique that eliminates the need for the computation of $R(\tau)$ is based on the following $k$th order difference [15]:

$$d(n) = x(n) - x(n-k) \tag{6}$$

which is zero for $k = 0, \pm p, \pm 2p...$ when the signal $x(n)$ is truly periodic with period $p$. This is clearly a faster method than most of the other period estimation techniques since it is just a difference equation. Now, by assuming that the sleep spindle segment of EEG is periodic, we can use a function of $d(n)$ to estimate the period

$$\gamma_n(k) = \sum_m |x(n+m)w_a(m) - x(n+m-k)w_b(m-k)| \tag{7}$$

which is referred to as the short-time Average Magnitude Difference Function (AMDF) [15]. One important feature of this function is that if the windows $w_a(m)$ and $w_b(m)$ are identical then it is indeed similar to the autocorrelation function [15]. Note that, the lower and upper boundries of (7) should be arranged properly when the data is of finite length.

In the study of experimental data in this paper, we use the following modified version:

$$D_n(k) = 1 - \frac{\gamma_n(k)}{\sum_i \gamma_n^2(i)} \tag{8}$$

which is similar to a normalized autocorrelation function and can be considered to be a second order statistical measure, where the term $\sum_i \gamma_n^2(i)$ is a normalization factor.

The inverse Fourier transform of the bispectrum $B(\omega_1, \omega_2)$, when calculated on one slice $\omega_1 = \omega_2 = \omega$, i.e.,

$$\begin{aligned} q(n) &= \frac{1}{2\pi}\int_{-\pi}^{\pi} B(\omega, \omega)e^{j\omega n} d\omega \\ &= \sum_m c(m, n-m) \end{aligned} \tag{9}$$

is called the sum-of-autotriplecorrelations (SOAT) [16]. Clearly, the SOAT in (9) are third order statistics and can be made similar to (2) and (8), i.e.,

$$\varphi_n(k) = \sum_{m=-M}^{M} |q(n+m)w(m) - q(n+m-k)w(m-k)| \tag{10}$$

and

$$Q_n(k) = 1 - \frac{\varphi_n(k)}{\sum_i \varphi_n^2(i)} \tag{11}$$

where $w(n)$ is, again, a window function and $M$ is an integer value defining the boundaries of the data segment, and the term $\sum_i \varphi_n^2(i)$ is the normalization factor.

We use the second and third order statistics (equations (8) and (11) respectively) together to estimate the periodicity of the spindle activity. If the spindle activity is purely periodic we expect these estimates to give similar results. If the results are not similar, then the existence of other linear or nonlinear relations are suggested. Moreover, the AMDF of SOAT in equation (11) can reveal background frequency sources even though other methods may under-estimate them.

## 3. COMPUTING METHODS

In practice, longer data is needed for meaningful bispectrum estimation [13]. We therefore group the EEG data over selected time segments (stages) for the frequency domain analysis. The set of electrodes are partioned into frontal, central and parietal subsets, i.e.,
`set C` = (`Cz, C1, C2, C3, C4, C5, C6`),
`set F` = (`Fz, F1, F2, F3, F4, F5, F6, F7, F8, F9, F10`),
`set P` = (`Pz, P1, P2, P3, P4, P5, P6, P7, P8, P9`).
(See: Figure 1 for the locations of the EEG electrodes.) While associating these neighboring electrodes, we visually evaluate the data. Moreover, we check for the results of commonly used second-order statistical classification methods such as correlation coefficients, ratio of harmonic energies, normalized bandwidths and mean frequencies [17]. Since approximately equivalent results are obtained, the channels are assumed to be associated adequately.

The estimation of the (averaged) normalized bispectrum is then accomplished for each group of channels sharing common features. These steps are itemized below:

- Apply a 256-point Hamming window to the EEG data to assure local stationarity.
- Remove the mean and estimate the bispectrum by the "direct method" [13].
- Repeat for all the members of the set and then average the bispectral values.
- Estimate the power spectrum of each segment and average them in a similar fashion.
- Mask the bispectral values below 10 % of the maximum peak value.
- Calculate the normalized bispectrum by using (5). Only the significant levels of normalized bispectrum ($b^2 > 0.1$) are considered for the evaluation of enery interaction among frequencies.

It is important to note that, the results are obtained over one triangular region $\omega_2 > 0$, $\omega_1 > \omega_2$ and $\omega_1 + \omega_2 < \pi$, simply because the bispectrum (normalized bispectrum) can be fully described over all frequencies by using the values in this region via its symmetry properties [13].

## 4. RESULTS

The top plots in Figure 1-(a) and (b) are segments of 8 seconds containing spindle activity. Visual evaluation and energy distribution of bandpass filtered data show that spindle activity starts approximately at sample point 1000 and ends at 1400 both for Cz and Pz channels.

In Figure 2-(a) and (b), a 1 second time region (between samples $1135$ to $1390$) where spindle activity is in progress is shown for Cz and Pz. The second order time-domain estimates (the middle plots of Figure 2) are similar for these channels. This suggests that any second order method (e.g., autocorrelation or power spectrum) will yield similar results in this segment. However, when we examine the third order estimates (the bottom plots of Figure 2), it may be seen that the results for Cz and Pz are different. When the window is moved forward to cover samples $1198$ to $1453$ the second and third order estimates have similar results as shown in Figure 3-(a) and (b) consistent with the observed steady-state oscillation in all channels.

The averaged normalized bispectra[1] of `set C` and `set P` from sample $1135$ to $1390$ are given in Figures 4-(a) and (b), respectively. In Figure 4-(a), for `set C`, the frequency regions at $(f_1, f_2)$ where $f_1 = 12 \sim 14$ and $f_2 = 1 \sim 2$ Hz; $f_1 = 6 \sim 9$ and $f_2 = 4 \sim 6$ Hz; $f_1 = 12 \sim 14$ and $f_2 = 13 \sim 14$ Hz; and finally $f_1 = 1.5$ and $f_2 = 4.5$ Hz show strong (almost unity) quadratical interactions. The results related with `set P` is given in Figure 4-(b). It is clear that for this time period, this region of brain is highly dominated by the spindle activity. However, the normalized bispectrum suggests that it would be more realistic to think that the sleep spindle activity has at least some types of second order nonlinearity (due to the appearance of the strong interactions in the $f_1 = 13 - 15$ and $f_2 = 12.5 - 14$ Hz region).

We show the contour plots of the averaged normalized bispectra for `set C`, and `set P` when the window is moved forward to cover samples $1198$ to $1453$ in Figure 5-(a) and (b), respectively. The normalized bispectra, when compared to Figure 4-(a) indicate relatively weaker quadratical interactions in the $(f_1 + f_2) \approx 13$ Hz line. The normalized bispectrum related with `set P` confirms that the spindle activity is dominating this region of brain with showing small interactions with other lower frequency components.

## 5. CONCLUSION

We have investigated time and frequency domain methods for analyzing sleep spindles. The time domain methods depend on the combination of second and third order statistical tools to detect the oscillatory dynamics of the spindle activity. In particular, we used two types of estimates: the autocorrelation and average magnitude differentiated sum-of-autotriplecorrelations. If both of these second and third order methods exhibit similar periodic behavior then we conclude that only "stationary" spindle activity exists. However, if they are different then the data has some influence from other (linear or nonlinear) activities which may occur due to complexities within this particular frame [18]. The existence of a nonlinearity has been tested via the bispectral analysis of EEG which characterizes the interaction of activity (within selected EEG segments) for different frequencies. For the frequency domain method, we have summarized the estimation method of the normalized bispectrum and discussed the issues of detecting those quadratic couplings which may occur due to existing nonlinearities. We have applied the bispectral techniques to adequately grouped EEG sleep stages and different epochs of various EEG sleep recordings. Our results suggest that, during sleep spindle activity, some types of nonlinearities exist. However, since our tests were limited to identifying second order nonlinearities, the existence of higher-order ($> 2$) nonlinearities may be checked in the future for all possible orders of the normalized higher-order spectra.

[1] For visualization purposes, the values are normalized with respect to the peak value and the normalized bispectrum is shown only within the half of the triangular region.

## 6. ACKNOWLEDGEMENT

The first author's work is supported in part by TÜBİTAK-BAYG and NATO Postdoctoral Fellowship while he was on leave from Çukurova University, Adana, Turkey. The authors would like to thank TÜBİTAK-BAYG and A. Hamit Serbest of Çukurova University for their support and encouragement.

## 7. REFERENCES

[1] R. M. Harper, R. J. Sclabassi & T. Estrin, "Time Series Analysis and Sleep Research," *IEEE Trans. Autom. Contr.*, Vol. AC-19, No. 6, pp. 932-943, 1974.

[2] A. A. Borbely & P. Achermann, "Concepts and Models of Sleep Regulation: An Overview," *J. Sleep Res.* 1, pp. 63-79, 1992.

[3] E. Niedermeyer & F. E. Lopes da Silva, (editors), *Electroencephalography*, Williams and Wilkins, Baltimore, 1993.

[4] M. Steriade, E. G. Jones & R. R. Llinas, *Thalamic Oscillations and Signaling*, John Wiley and Sons, NY, 1990.

[5] J. Marc, E. Poiseau, P. Jähnig, H. Schulz & S. Kubicki, "Topographical Analysis of Sleep Spindle Activity," *Neuropsychobiology*, 26, pp. 210-217, 1992.

[6] M. Sun, S. Qian, X. Yan, S. B. Baumann, X. Xia, R. E. Dahl, N. D. Ryan & R. J. Sclabassi, "Localizing Functional Activity in the Brain Through Time-Frequency Analysis and Synthesis of the EEG," *Proc. IEEE*, Vol. 84, No. 9, pp. 1302-1311, 1996.

[7] T. P. Barnett, L. C. Johnson, P. Naitoh, N. Hicks & C. Nute, "Bispectrum Analysis of Electroencephalogram Signals during Waking and Sleeping," *Science*, Vol. 172, No. 3981, pp. 401-402, 1971.

[8] G. Edlinger, C. Andrew & G. Pfurtscheller, "Second Order and Third Order Statistics with Application to EEG," *Proc. of IEEE Medicine and Biology Conference* (in CD), 1995.

[9] T. Ning & J. D. Bronzino, "Bispectral Analysis of the Rat EEG During Various Vigilance Stages," *IEEE Trans. Biomed. Eng.*, Vol. 36, No. 4, pp. 497-499, 1989.

[10] D. L. Sherman & M. D. Zoltowski, "Decomposing the Alpha Rhythms: Comparative Performance Evaluation of Parametric Bispectral Algorithms for EEG," *IEEE Proceedings of 6th SSAP Workshop*, pp. 522-525, 1992.

[11] T. Ning & J. D. Bronzino, "Nonlinear Analysis of the Hippocampal Subfields of CA1 and the Dentate Gyrus," *IEEE Trans. Biomed. Eng.*, Vol. 40, No. 9, pp. 870-876, 1993.

[12] D. R. Brillinger, "An Introduction to Polyspectra," *Ann. Math. Stat.*, Vol. 36, pp. 1351-1374, 1965.

[13] C. L. Nikias & A. Petropulu, *Higher-Order Spectra Analysis: A Nonlinear Signal Processing Framework*, Prentice Hall, NJ, 1993.

[14] T. S. Rao, “Bispectral Analysis of Nonlinear Stationary Time Series,” in *Handbook of Statistics 3*, D. R. Brillinger and P. R. Krishnaiah (editors), North Holland, 1983.

[15] L. R. Rabiner & R. W. Schafer, *Digital Processing of Speech Signals*, Prentice-Hall, NJ, 1978.

[16] T. Akgül & A. El-Jaroudi, “Reconstruction of Mixed-Phase Signals from Sum-of-Autotriplecorrelations,” *IEEE Trans. Signal Processing*, Vol. 46, No. 1, pp. 250-254,1998.

[17] R. J. Sclabassi, M. Sun, D. N. Krieger, P. Jasiukaitis & M. S. Scher, “Time-Frequency Domain Problems in the Neurosciences,” in *Time-Frequency Signal Analysis: Methods and Applications*, B. Boashash (editor), Longman-Cheshire, pp. 498-519, 1992.

[18] E. Başar, (editor), *Chaos in Brain Function*, Springer-Verlag, Berlin, 1990.

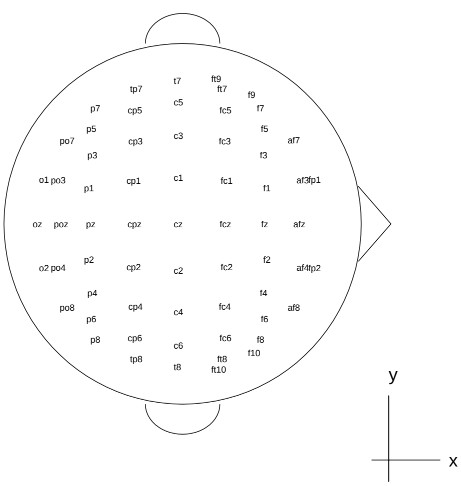


Figure 1: Location of 64 recording electrodes utilized in obtaining the data in this paper.

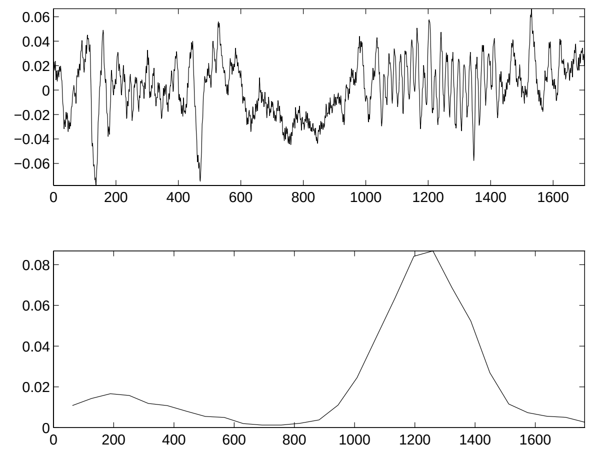

(a) Eight seconds of Cz data (top), its energy distribution after bandpass filtering (bottom).

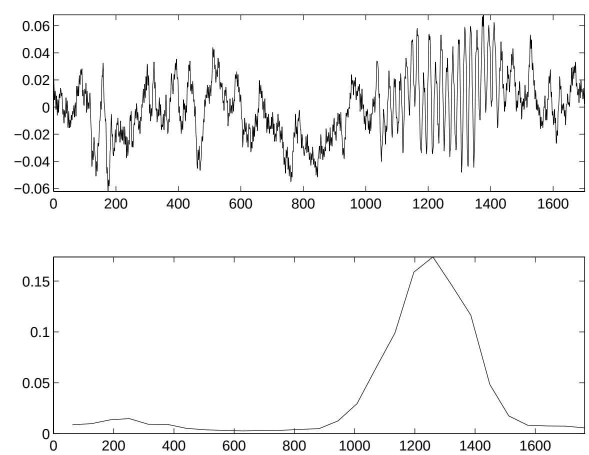

(b) Eight seconds of Pz data (top), its energy distribution after bandpass filtering (bottom).

Figure 2: Raw EEG samples of Cz and Pz (top plots) and after applying a bandpass (8-15 Hz) filter to each channel, their energy distributions over samples (bottom plots) in (a) and (b), respectively.

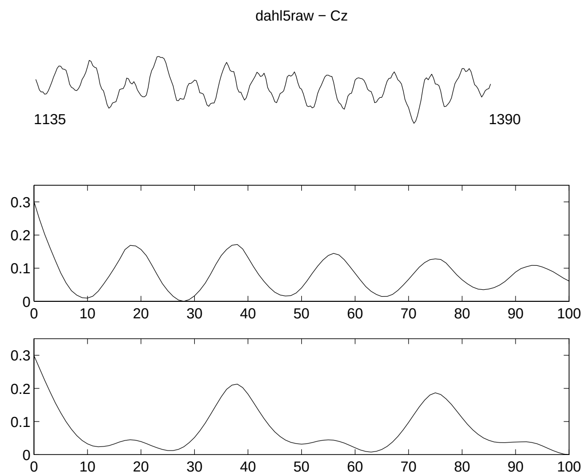


(a) Data segment of Cz (top), ADMF (middle) and ADMF of SOAT of the sleep spindle data.

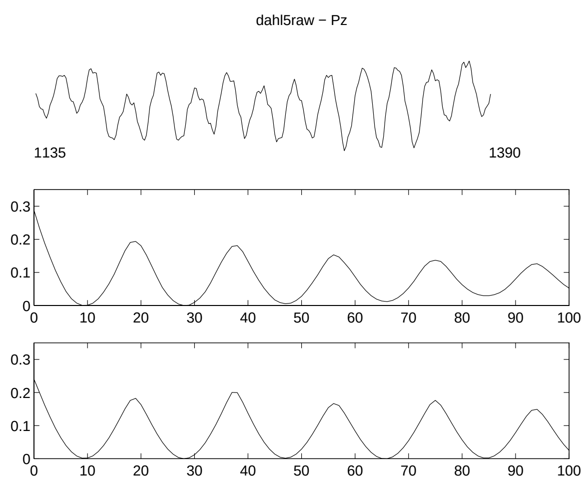


(b) Data segment of Pz (top), AMDF (middle) and AMDF of SOAT of the sleep spindle data.

Figure 3: EEG segments of Cz and Pz from samples 1135 to 1390 (top plots), AMDF measurements (middle plots), AMDF of SOAT of data with lag 100 (bottom plots) in (a) and (b), respectively.

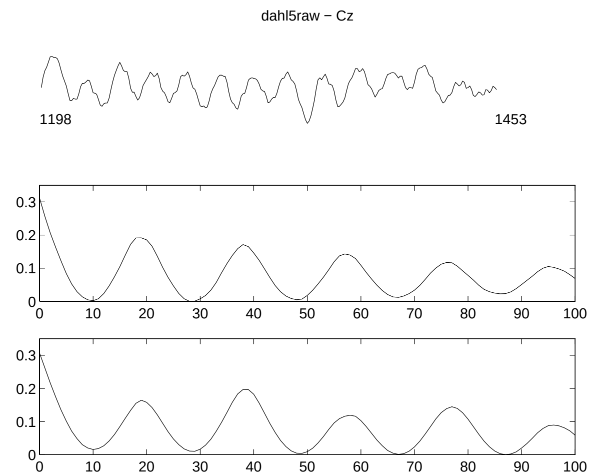


(a) Data segment of Cz (top), ADMF (middle) and ADMF of SOAT of the sleep spindle data.

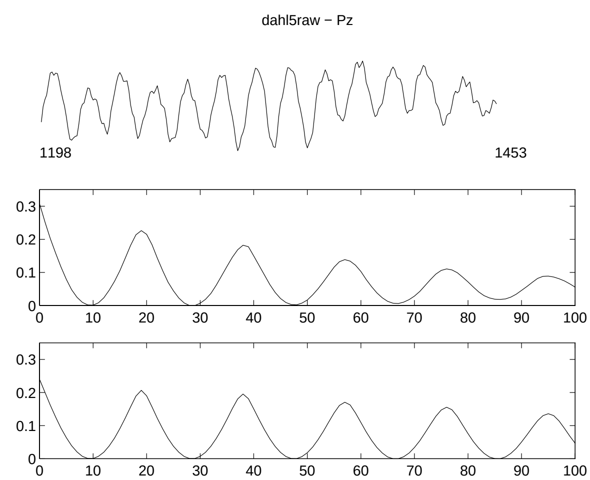


(b) Data segment of Pz (top), AMDF (middle) and AMDF of SOAT of the sleep splindle data.

Figure 4: EEG segments of Cz and Pz from samples 1198 to 1453 (top plots), AMDF measurements (middle plots), AMDF of SOAT of data with lag 100 (bottom plots) in (a) and (b), respectively.

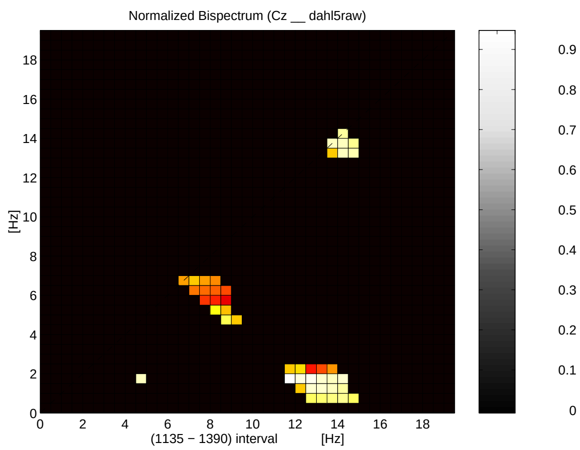


(a) Image view of the normalized bispectrum for set C.

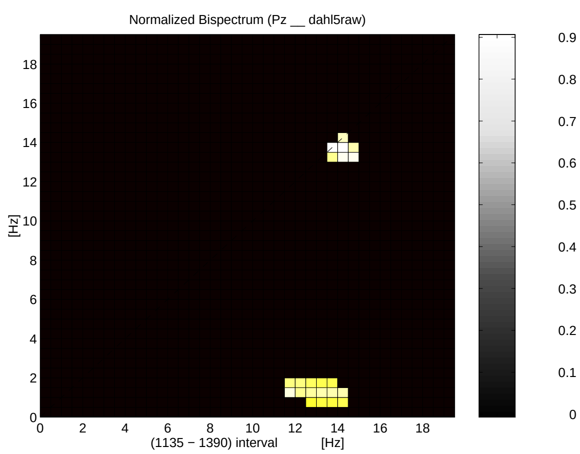


(b) Image view of the normalized bispectrum for set P.

Figure 5: Image view of the normalized bispectrum from samples 1135 to 1390: (a) for set C; (b) for set P.

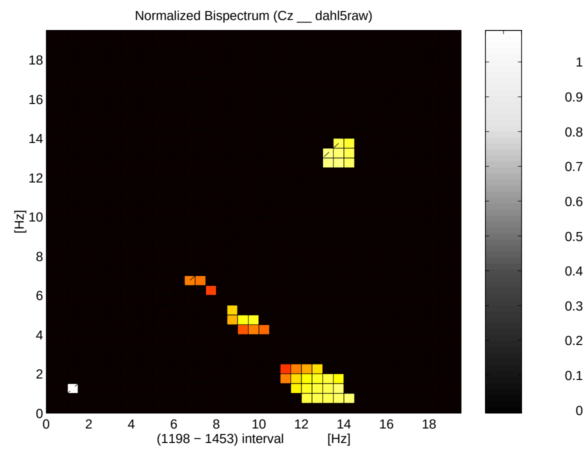


(a) Image view of the normalized bispectrum for set C.

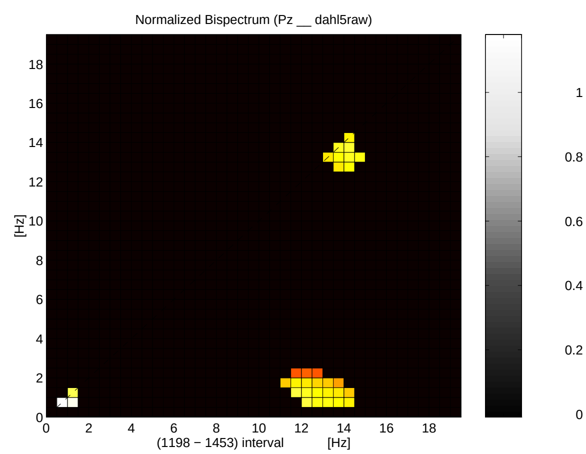


(b) Image view of the normalized bispectrum for set P.

Figure 6: Image view of the normalized bispectrum from samples 1198 to 1453: (a) for set C; (b) for set P.